COMPONENT PART NOTICE

THIS PAPER IS A COMPONENT PART OF THE FOLLOWING COMPILATION REPORT:

(TITLE): Proceedings of the Workshop on Unsteady Separated Flow Held at the United States Air Force Academy on A ugust 10 11, 1983.

(SOURCE): Air Force Office of Scientific Research, Bolling AFB, DC. Directorate of Aerospace Sciences.

TO ORDER THE COMPLETE COMPILATION REPORT USE AD-A148 249.

THE COMPONENT PART IS PROVIDED HERE TO ALLOW USERS ACCESS TO INDIVIDUALLY AUTHORED SECTIONS OF PROCEEDINGS, ANNALS, SYMPOSIA, ETC. HOWEVER, THE COMPONENT SHOULD BE CONSIDERED WITHIN THE CONTEXT OF THE OVERALL COMPILATION REPORT AND NOT AS A STAND-ALONE TECHNICAL REPORT.

THE FOLLOWING COMPONENT PART NUMBERS COMPRISE THE COMPILATION REPORT:

AD#:	TITLE:
AD P004 153	Supermaneuverability.
AD-P004 154	Wing Rock Flow Phenomena.
AD-P004 155	Potential Applications of Forced Unsteady Flows.
AD-P004 156	Unsteady Stall Penetration of an Oscillating Swept Wing.
AD-P004 157	Simultaneous Flow Visualization and Unsteady Lift Measurement on an Oscillating Lifting Surface.
AD-P004 158	A Visual Study of a Delta Wing in Steady and Unsteady Motion.
AD-P004 159	Comparative Visualization of Accelerating Flow around Various Bodies, Starting from Rest.
AD-P004 160	Prediction of Dynamic Stall Characteristics Using Advanced Nonlinear Panel Methods.
AD-P004 161	Numerical Solution of the Navier-Stokes Equations for Unsteady Separated Flows.
AD-P004 162	Unsteady Aerodynamic Loading of an Airfoil due to Vortices Released Intermittently from Its Upper Surface.
AD-P004 163	A Navier-Stokes Calculation of the Airfoil Dynamic Stall Process.
AD-P004 164	Some Structural Features of Unsteady Separating Turbulent Shear Flows.
AD-P004 165	Can the Singularity Be Removed in Time-Dependent Flows?
AD-P004 166	On the Shedding of Vorticity at Separation.
AD-P004 167	Unsteady Separated Flows. Forced and Common Verticity about Oscillating Airfoils.
AD-P004 168	Unsteady Separated Flows. Generation and Use by Insects.
AD-P004 169	Theoretical Study of Non-Linear Unsteady Aerodynamics of a Non-Rigid Lifting Body.

DTIC
S DEC 1 4 1984
A

This document has been approved for public release and sale; its distribution is unlimited.

Distribution/
Availability Codes
Dist | Avail and/or Special
A-1

COMPONENT PART NOTICE (CON'T)

AD#:	TITLE:
AD-P004 170	Theoretical Investigation of Dynamic Stall Using a Momentum Integral Method.
AD-P004 171	Preliminary Results from the Unsteady Airfoil Model USTAR2.
AD-P004 172	Experiments on Controlled, Unsteady, Separated Turbulent Boundary Layers.
AD-P004 173	Genesis of Unsteady Separation.
AD-P004 174	Flow Separation Induced by Periodic Aerodynamic Interference.
AD-P004 175	Leading Edge Separation Criterion for an Oscillating Airfoil.
AD-P004 176	Natural Unsteadiness of a Separation Bubble behind a Backward-Facing Step.

FLOW SEPARATION INDUCED BY PERIODIC AERODYNAMIC INTERFERENCE

E.E. Covert*, P.F. Lorber**, and C.M. Vaczy**

Department of Aeronautics and Astronautics
Massachusetts Institute of Technology
Cambridge, MA 02139

AD-P004 174

ABSTRACT

Analysis of experimental surface pressure distributions on a NACA 0012 airfoil has revealed four flow states: attached, separated, borderline, and dynamically separated. The important parameters that determine the flow state are Reynolds number, reduced frequency, airfoil angle of attack, and surface condition at the leading edge. Testing was done at Re=700,000, .5<=k<=6.4, and 0<=alpha<=18 degrees. For this flow the dynamically separated state takes the form of an alternation between attached and separated flow. It has a period that ranges from 1 to 30 times that of the unsteady perturbation. In the separated state a convected surface pressure disturbance was identified, and found to propagate downstream from a location near the leading edge at a phase speed of 1/3 to 1/2 that of the freestream velocity.

INTRODUCTION

The efficient design of all aerodynamic devices depends on a fundamental understanding of the surrounding flow field. A steady unseparated flow field can usually be accurately modelled. If unsteady and/or separated boundary layers are present, as is the case in the flow around helicopter rotors and inside gas turbine engines, the problem becomes much more complicated.

The present experiment uses a rotating elliptic cylinder to generate unsteady flow on a NACA 0012 airfoil. The elliptic cylinder, located behind and beneath the trailing edge of the airfoil, induces a periodic change in angle of attack of attack at the trailing edge, as well as a small induced periodic flow curvature. This apparatus has been used previously to study unsteady airfoil pressures, boundary layers, and wakes(1,2,3). Analysis of airfoil surface pressure distributions and boundary layer velocity profiles suggests four flow states: the attached state, the separated state, the borderline state, and the dynamically separated state. Different ranges of Reynolds number, reduced frequency, and airfoil angle of attack can be combined to produce any one of the four flow states around the airfoil. The conditions under which the airfoil is in s given state differ dramatically from the conditions for the steady state airfoil (normally stall is at 16 degrees in a uniform field).

EXPERIMENT

As shown on figure 1, the airfoil, which has both span and chord equal to 50.8 cm, is mounted at fixed angle of attack between 2 vertical sidewalls in the test section of the MIT Wright Brothers Memorial Wind Tunnel. Although air speeds of 1 to 90 mps are available, most of the data reported here were taken at 20 mps, corresponding to a Reynolds number based on airfoil chord of 700,000. For these tests the elliptic cylinder (semi-axes of 0.136 and 0.061 chord) is located at x/c=0.120, y/c=-.190, as measured from the airfoil trailing edge to the ellipse axis of rotation. This distance is the same for all airfoil angles of attack. The ellipse can be held steady with its major axis either horizontal or vertical, or rotated clockwise at up to 3300 rpm. At 20 mps, this corresponds to a range of reduced frequencies, $k=\omega c/2U_\infty$, between 0 and 8.2.

Airfoil pressures are measured at 77 locations on the surface. The 19 taps along the centerline of each surface between x/c=.0 and x/c=0.98 are the primary set, while additional taps at spanwise locations z/c=+-0.125 and +-0.250 are used to check two-dimensionality. Each pressure tap is connected to a pressure transducer via an individually tuned 10cm tube and a Scanivalve pressure scanner. The frequency response of this system has been calibrated as described in reference 1, giving an estimated accuracy in amplitude of +-1% for frequencies < 50 Hz and +- 3% for 75Hz < f < 150 Hz.

Data may be either recorded using an analog FM tape recorder or digitized by an online computer. The computer system, diagrammed in figure 2, is used to form the ensemble average of the pressure coefficient, based upon 100 to 2048 ellipse rotation periods. These averages are stored on disc and may later be Fourier transformed to determine the amplitude and phase lag at the fundamental frequency and at its harmonics, along with the mean. Phase lag is defined so that a phase lag of 0 degrees implies that the minimum of the signal occurs when the ellipse is horizontal, while 180 degrees implies a delay of the minimum until the ellipse axis is vertical. Phase lags are estimated to be accurate to +-3 degrees for frequencies less than 100 Hz.

In addition to the three previously mentioned independent variables (Re,k and alpha),there is one variable surface condition: either a smooth leading edge with natural boundary layer transition or a roughened leading edge with artificial boundary layer transition. The lesding edge is roughened by applying a thin (2mm)line of #120 grit. The grit causes an earlier boundary layer transition on the upper surface, and often has a major effect on the separation behavior.

---

* Professor of Aeronautics and Astronautics
** Research Assistant

EXPERIMENTAL RESULTS

THE BOUNDARY LAYER WITH NATURAL TRANSITION

The attached flow regime includes, at a Reynolds number of 700,000, all of the studied reduced frequencies($k \leq 6.4$) up to an angle of attack of 10 degrees. In the above defined range there are only three cases in which the flow is not fully attached. The first is a possible laminar separation bubble located just downstream of the suction pressure peak. This small bubble extends over not more than 2% of the chord and does not appear to be greatly affected by reduced frequency. Stretford's method for laminar boundary layers predicts separation for the airfoil alone at 10 degrees to be at $x/c=.03$, while oil flow visualization shows that the bubble starts at about $x/c=.02$, and extends to $x/c=.04$. Stratford's method does not predict the global separation of the boundary layer, but the approximate location of the start of the separation bubble. The second case is a trailing edge separation zone which, if present, extends over not more than the last 5 % of the chord. The third case, occurring at an angle of attack of 10 degrees and a reduced frequency of 6.4, is an example of the borderline flow state, and will be discussed below.

The attached state also exists at higher angles of attack, but the reduced frequency for which it exists decreases as angle of attack increases. By alpha=14 degrees, the only attached case is one in which the ellipse is in the steady horizontal position. For all measured values of reduced frequency the upper surface boundary layer is separated. Figure 3 shows, for alpha=10 degrees, the mean pressure coefficient versus distance for the measured values of reduced frequency. As reduced frequency is increased, there is not only an overall increase in the mean difference pressure coefficient, but also a dramatic increase in the mean pressure coefficient at the leading edge suction peak. This increase is due to the increase in mean circulation added by the rotating ellipse. Once this peak obtains a value of about -6.2, the corresponding adverse pressure gradient over the bubble has become too large for the boundary layer to reattach, and so the entire boundary layer separates.

The borderline regime studied includes a small band of reduced frequencies at each angle of attack between 10 and 14 degrees. A typical example occurs at alpha = 10 degrees, k= 6.4. The upper surface boundary layer can remain indefinitely attached until it is upset by a large enough random wind tunnel disturbance. Once the boundary layer is disturbed, it will separate, and will remain separated indefinitely. To get the flow to reattach, the reduced frequency must be lowered to about k=1.0. This type of hysteresis is typical of separated flows(4). Figure 4 shows a comparison of the mean pressure distributions for both k=6.4 cases. Although the upper surface pressure coefficient has been totally changed by the separation of the boundary layer, the lower surface pressure coefficients are almost identical. Figure 5 shows a comparison of the amplitude at the fundamental frequency for both cases. As is true for the mean pressure coefficient, the upper surface pressure coefficients at the fundamental harmonic are quite different, while the lower surface coefficients are very similar. Although the difference in mean pressure coefficient (lower-upper surface) in the attached case is generally much higher than that in the separated case, the amplitude of the difference in the unsteady pressure coefficient at the fundamental frequency is generally higher for the separated case.

As the angle of attack increases, the reduced frequency for which the borderline case exists decreases. Figure 6 shows a map of alpha -vs- k for the different flow states at a Reynolds number of 700,000.

The separated flow regime includes, for alpha $\geq$ 14 degrees, all unsteady cases, plus the steady case of the vertical ellipse. It also includes the band from 10 degrees $\leq$ alpha $\leq$ 14 degrees shown in Figure 6. The separation is a leading edge separation caused by the bursting of the leading edge separation bubble. The separation zone includes all of the upper surface, and even a small region ahead of the stagnation point on the lower surface. The pressures, although usually random in appearance due to large aperiodic fluctuations, may in fact have an even higher ensemble averaged amplitude at the fundamental frequency than the pressures in the attached flow. Figure 5 shows this for the borderline state cases at alpha=10 degrees, k=6.4.

Figure 7 shows a plot of the mean pressure coefficients for the case alpha=15 degrees. Unlike the mean pressure coefficient for the attached flow (figure 3), the mean pressure coefficient for the separated flow does not steadily increase near the suction peak as reduced frequency increases. The mean pressure coefficient over the entire upper surface follows no obvious pattern as a function of reduced frequency.

The dynamically separated regime includes a small band for alpha $\geq$ 10 degrees, $k < .5$. This is an unsteady special case of the borderline state. To locate this state for a fixed alpha, k and Re are varied until the flow on the upper surface alternates between the attached and the separated states. The number of ellipse periods spent in each state varies considerably, but in general is between 1 and 30. The flow on the lower surface reacts to the flow on the upper surface with a phase difference (either lead or lag) of approximately 15 deg or less. Figure 8 shows, for alpha=12.5 degrees, and Re=1,100,000, typical unaveraged traces of the upper and lower surface pressures at $x/c=.005$. Note the increased periodicity of the attached flow compared to that of the separated flow. The separated flow may attempt to reattach as the ellipse passes through the horizontal position. Sometimes it suceeds, while other times it does not.

THE EFFECT OF ARTIFICIAL TRANSITION ON THE BOUNDARY LAYER

The effect of leading edge roughness on the boundary layer is quite significant. At angles of attack for which the leading edge separation bubble would naturally be present, the addition of the grit causes an artificial transition upstream of the separation bubble location. This results in the bubble not forming, and thus there is a net increase(by up to 10 %) in mean lift when grit is used. Figure 9 shows a comparison, for alpha=10 degrees,k=1.0 of the mean pressure coefficients for the smooth surface and rough surface cases. Note that the two cases are not at any one position substantially different, but instead differ slightly over the entire chord.

A second, rather dramatic, effect of the added roughness is to delay, in terms of alpha and k, the separation of the upper surface boundary layer. Figure 10 shows a plot of the location in k - alpha space of the different flow regimes with leading edge roughness present. This plot is qualitatively similar to that for the smooth surface case, figure 6, although the flow state bands are offset to a higher reduced frequency at each alpha.

The mean pressure coefficients at alpha=12 degrees for various values of reduced frequency are shown in figure 11. The boundary layer at low to moderate reduced frequencies (k<=3.2) remains attached over the entire surface (possibly excluding the trailing edge). As k increases, the upper surface boundary layer separates. A relatively small adjustment in k (from 4.0 to 3.2) will cause the boundary layer to reattach. The hysteresis loop is much smaller than that in the case of natural transition. Figure 12 shows a plot similar to figure 11, but for alpha=14 degrees. At this angle of attack, the boundary layer is no longer fully attached for the lowest measured value of reduced frequency. The attached region is reduced at k=1.0 to a narrow strip from the leading edge to about x/c=.1. Based upon figures 11 and 12, the behavior of the boundary layer can be summarized as follows: as reduced frequency is increased, the upper surface boundary layer changes from being attached, to being partially attached, to being fully separated. This is the pattern that was observed during testing and also recorded on tape.

By looking again at figure 11, it is seen that when the flow is attached the mean pressure coefficient follows the same trend as in the smooth leading edge case:it steadily becomes more negative at the suction peak as reduced frequency increases. The value of the mean pressure coefficient at the suction peak that can now be reached before separation has been increased to -7.0(versus -6.2). Once the flow has separated, the mean pressure coefficient does not steadily increase with increasing k (same behavior as for the smooth leading edge case).

The artificial roughness also changes the type of separation on the airfoil. With a smooth leading edge, the separation seems to be a laminar leading edge separation caused by the leading edge separation bubble bursting, but with artificial roughness the flow has a trailing edge separation that rapdily makes its way to a station close to the leading edge. The failure of the roughened leading edge boundary layer to separate under the same conditions that cause separation with a smooth leading edge leads to the conclusion that the separation with a smooth leading edge is a laminar bubble burst and not a turbulent separation. Since the boundary layer under the roughened leading edge condition separates downstream of the suction pressure peak, it is likely that the separation originates at the trailing edge, and again is not a turbulent leading edge separation.

For the boundary layer that has undergone transition artificially, dynamic separation is still evident, but it is noticeably changed. Without the trip, the boundary layer is either fully separated or fully attached (excluding the trailing edge separation zone and the leading edge separation bubble). When the trip is used, the boundary layer can at a given time be in any one of the following three states: upper surface fully attached, upper surface partially attached/partially separated, or upper surface fully separated. The flow may alternate between all three conditions, of just the latter two conditions, depending on the angle of attack, reduced frequency, and Reynolds number. This seems to indicate that the roughness changes the nature of the dynamic separation from that caused by a separation bubble alternately reattaching or not reattaching to that caused by a trailing edge separation zone that moves,in no known order, between being near the trailing edge, near the leading edge on the lower surface, or a short distance downstream of the leading edge (about x/c=.1 for alpha=14 degrees,k=2.0). Figure 13 shows typical unaveraged pressure traces for dynamic separation in the case with a roughened leading edge at alpha=15 deg,Re=700,000,k=4.2. The flow at the leading edge tap is sometimes separated, and sometimes attached. The unsteady component of the attached flow no longer appears to be more periodic than that in the separated flow. The mean value of the pressure must also be considered in the determination of the flow state. This is due to the large amount of separated flow, downstream of the attached leading edge, that influences the flow field ahead of the separation point.

DISCUSSION OF RESULTS

Figure 14 shows the phase lags at the fundamental frequency for alpha=10 degrees, k=6.4 for both the attached and separated states. The pressure distribution for the attached boundary layer primarily exhibits a standing wave behavior (nearly constant phase lag) over the upper and lower surfaces, with the exception of the leading and trailing edges. In general for all the attached cases studied so far, if nonconstant phase lags exist over substantial portions of the upper surface(not just at the leading or trailing edge), the source is the trailing edge (i.e. the phase lag

is at a minimum at the trailing edge). The pressure distribution of the separated boundary layer, although virtually unchanged on the lower surface, now exhibits an added convected behavior on the upper surface. Unlike the attached state, the convected effect now appears to originate at a location near the leading edge.

Figure 15 shows, for alpha=15 degrees, the phase lag at the fundamental frequency for all studied values of reduced frequency. At low reduced frequency (k<=.5) the pressure disturbance originates near the leading edge and moves downstream over the first 70% of the upper surface. A disturbance originating at the trailing edge propagates upstream over the last 10% of the upper surface. At moderate values of reduced frequency (1.0<=k<=2.0) the disturbance originating at the trailing edge is no longer present. The disturbance originating near the leading edge seems to propagate over the entire upper surface. At high values of reduced frequency (k>=3.9) the disturbance originating at the trailing edge reappears, and now propagates over approximately 50% of the upper surface. The disturbance originating near the leading edge now propagates over less than 50% of the upper surface. The middle region may be referred to as an "interference region" between the disturbances traveling in opposite directions. This region is also observed for low values of reduced frequency, but not for moderate values of reduced frequency.

A related effect was reported in reference 5. A NACA 0012 airfoil was held steady above the stall angle, and the propagation of individual pressure disturbances was observed using surface pressure transducers. Disturbances propagated upstream on the pressure surface, were reversed in phase by 180 degrees at the stagnation point, and were then convected downstream on the first 2/3 of the suction surface at nearly the freestream velocity.

From the plots of phase lag of the fundamental frequency, an average value of the phase velocity can be calculated by fitting a least squares line through the data. Figure 16 shows typical phase lag plots at alpha=14 degrees, k=2.0, for both the natural and artificial transition cases. As can be seen in figure 16 ,the use of the boundary layer trip has little effect on phase velocity. Although the least squares line is offset due to different leading edge effects, the slope for the rough leading edge case is only 3% lower than that for the smooth leading edge case. Figure 17 shows the variation of phase velocity with reduced frequency and angle of attack. It is apparent from the figure that phase velocity is strongly dependent on reduced frequency, while only mildly dependent on angle of attack. Within a band of +-5% of the freestream velocity, the average phase velocity may be approximated by V/Ui = .35+.023k. The two cases at k=2 that have a higher phase velocity are as yet unexplained.

Returning to figure 5 (amplitude at alpha=10 degrees, k=6.4), one realizes that the upper surface amplitude for the separated state can be divided into two parts. The first component increases smoothly with x and is only slightly larger than the amplitude in attached flow. This seems to indicate that this standing wave like contribution is relatively independent of the flow state. The second contribution is a damped oscillation in x, and is related to the convected behavior seen in the phase lag. Both effects are seen on the same portions of the airfoil, and both oscillate with similar periods in x. On the lower surface, the amplitude of the pressure coefficient at the fundamental frequency is basically the same for both states, with the separated state having a slightly higher value.

Figure 18 shows the amplitude at the fundamental frequency for the same cases as in figure 15 . At low reduced frequencies the amplitude increases monotonically until the interference region. After this region it decreases rapidly. For moderate reduced frequencies the amplitudes do not tend to decrease, but rather fluctuate in x over the entire upper surface. At high reduced frequencies the oscillation amplitude peaks quickly, and is then damped. The damping is increased as reduced frequency is increased. The lower reduced frequency cases also exhibit damping, but since the initial oscillation amplitudes are not as great, the damping is not as noticeable. The basic character of the lower surface amplitude is not affected by reduced frequency, although the magnitudes change.

Figure 19 shows, for alpha=14 degrees, k=6.4, the amplitudes at the fundamental frequency for both the natural transition case and the artificial transition case. Without the boundary layer trip, the initial amplitude of the disturbance is much larger by a factor of 1.5, but the damping ratio is much higher, 6.1 versus 4.0. This results in the amplitudes being very similar in the vicinity of the trailing edge. This trend seems typical of all such cases studied so far.

SUMMARY AND CONCLUSIONS

Four flow states have been identified to exist around the NACA 0012 airfoil in this unsteady flow field. The attached state always exists for low(<10 degrees) angles of attack. The separated state always exists for high(>16 degrees) angles of attack. At intermediate angles of attack, the flow state is highly dependent on reduced frequency. The use of a boundary layer trip at the leading edge changes the range of alpha for which each flow state exists.

The separated flow is characterized by a small, negative and nearly constant mean pressure coefficient on the upper surface. Part of the pressure field is in the form of a convected disturbance which originates near the leading edge of the airfoil, and moves downstream at an average phase speed of about one third to one half that of the freestream. The phase speed is not constant in x, as is apparent from the curvature in the phase plots. The disturbance amplitude is also not constant, as it oscillates in x. The amplitude is quickly amplified near the leading edge, and then slowly damped. The amplification and damping are

highly reduced frequency dependent. More work is needed to fully describe this behavior.

Dynamic separation is an unsteady state that alternates between the attached and separated states. With natural transition it has only been observed at low (<.5) values of reduced frequency. At moderate to high reduced frequencies a quasi-stable borderline state exists. The boundary layer can be either separated or attached, but it does not fluctuate between one or the other.

The use of a boundary layer trip significantly alters the stall characteristics of the airfoil. This is due to a change in the nature of the separation from a laminar leading edge separation(due to bubble burst), to a turbulent trailing edge separation. This allows the upper surface boundary layer to be not only fully attached or fully separated, but also to be partially attached.

When the boundary layer remains attached for a short distance on the upper surface, as is the case sometimes when the boundary layer trip is used, the disturbances are still amplified, but not nearly as much. This change is offset by a smaller damping ratio so that near the trailing edge the behavior becomes very similar. The average velocity of the disturbance is nearly the same for both cases.

Dynamic separation when the leading edge boundary layer trip is present is of a different form than that with no trip. The dynamic separation can now exist at moderate reduced frequencies as well as low reduced frequencies. The flow has a preferred condition, and will jump to the other conditions in an unpredictable order, and stay there generally from 1 to 10 ellipse periods. This change from the behavior of the case with natural transition is brought about by a change in the form of separation from one of a laminar bubble that alternately attaches or remains separated, to that of a quickly moving trailing edge separation point.

REFERENCES

1. Lorber,P.F. and Covert,E.E., "Unsteady Airfoil Pressures Produced by Periodic Aerodynamic Interference," AIAA Journal, vol.20, Sept. 1982,pp. 1153-59.

2. Covert,E.E. and Lorber, P.F., "Unsteady Turbulent Boundary Layers in Adverse Pressure Gradients," AIAA paper 82-0966,June 1982, accepted for publication in AIAA Journal.

3. Covert,E.E., Lorber,P.F. and Vaczy,C.M., "Measurements of the Near Wake of an Airfoil in Unsteady Flow," AIAA paper 83-0127, January 1983.

4. McCroskey,W.J., Carr,L.W. and McAlister,K.W., "Dynamic Stall Experiments on Oscillating Airfoils," AIAA Journal, vol. 14, Jan. 1976, pp57-63.

5. St. Hilaire,A.O., Carta,F.O., Fink,M.R. and Jepson,W.D., "The Influence of Sweep on the Aerodynamic Loading of an Oscillating NACA 0012 Airfoil," NASA CR-3092, May 1979.

Acknowledgement

This research is sponsored by the U.S. Air Force Office of Scientific Research under grant AFOSR-80-0282. Dr. Michael S. Francis is the contract monitor.

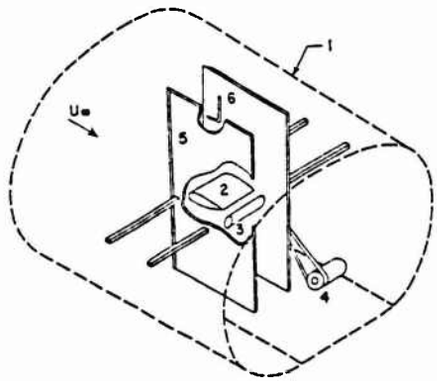

1) Test Section
2) NACA 0012 Airfoil
3) Rotating Elliptic Cylinder
4) Drive Motor (0-3300 rpm)
5) 2-D Sidewalls
6) Pitot-Static Probe

Fig. 1 Schematic of the test section for unsteady airfoil tests.

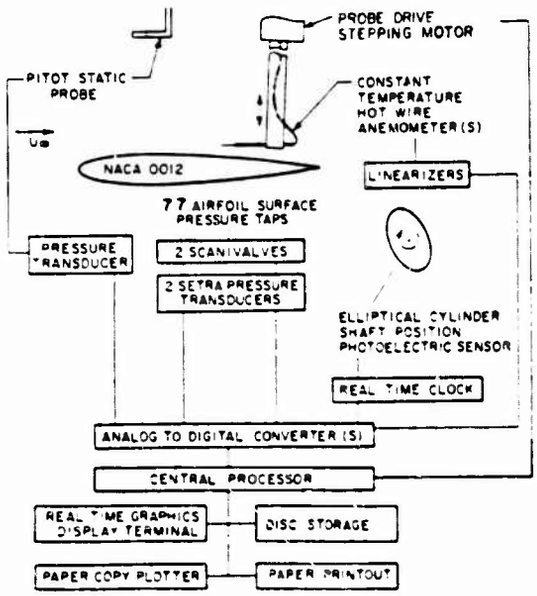

Fig. 2 Block diagram of the data acquisition system

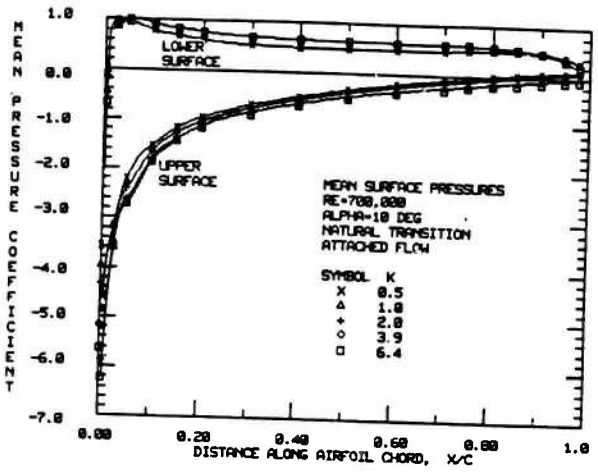

Fig. 3 Reduced frequency dependence of the mean pressures in attached flow.

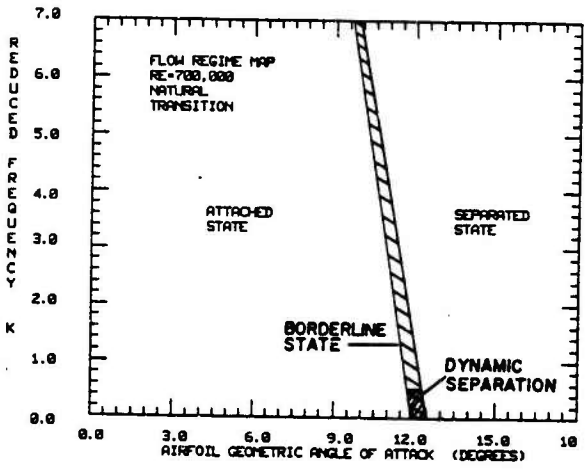

Fig. 6 Flow regime map for natural transition.

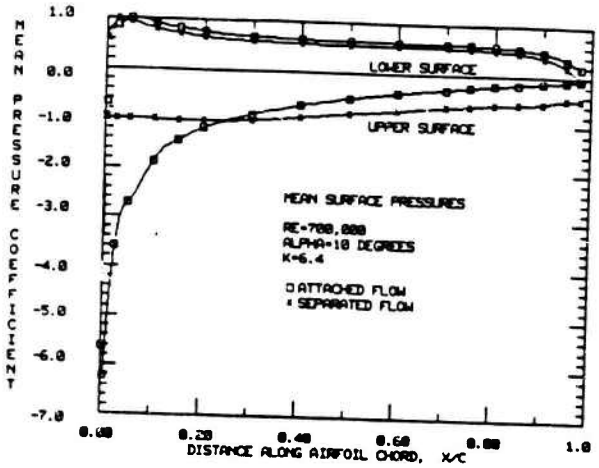

Fig. 4 Comparison of the mean pressure distribution in the attached and separated cases.

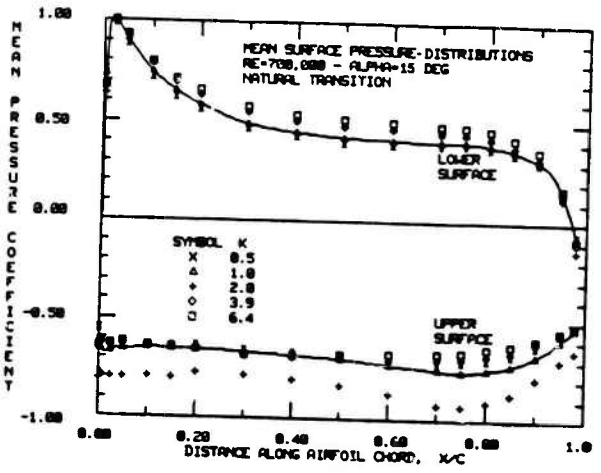

Fig. 7 Reduced frequency dependence of the mean pressures in separated flow.

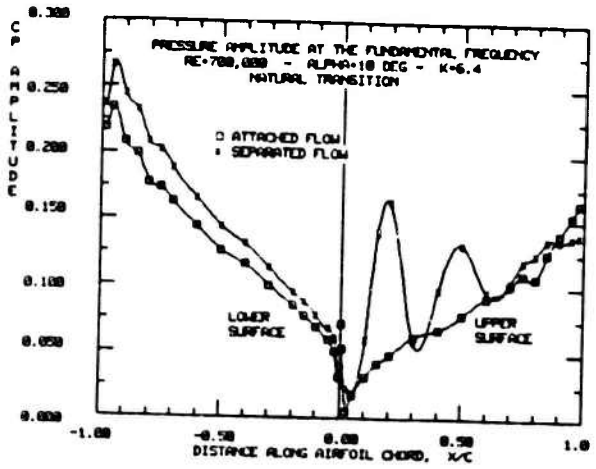

Fig. 5 Comparison of the unsteady pressure amplitudes in the attached and separated cases.

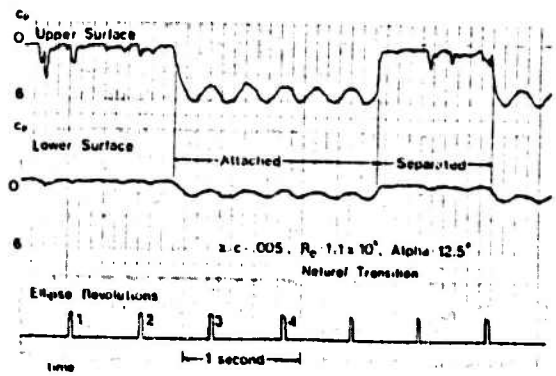

Fig. 8 Typical pressure variation with time for the dynamically separated state with natural transition.

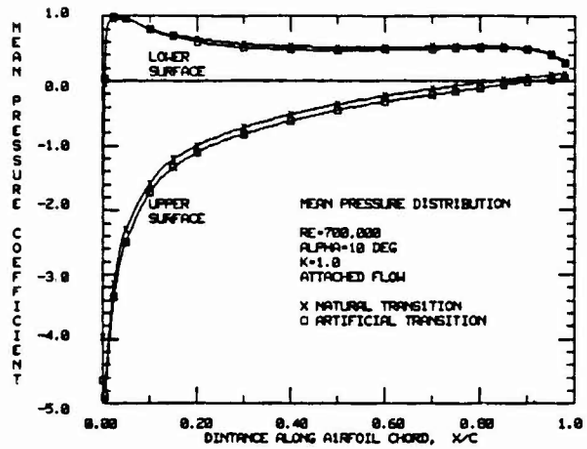

Fig. 9 Comparison of the mean pressure distributions for natural and artificial transition.

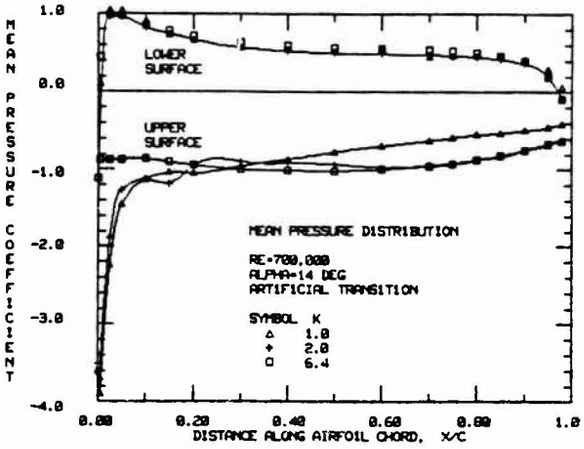

Fig.12 Reduced frequency dependence of the mean pressures at alpha=14 degrees.

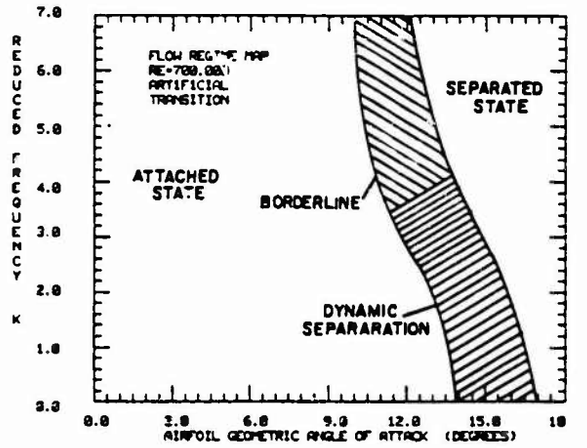

Fig.10 Flow regime map for artificial transition.

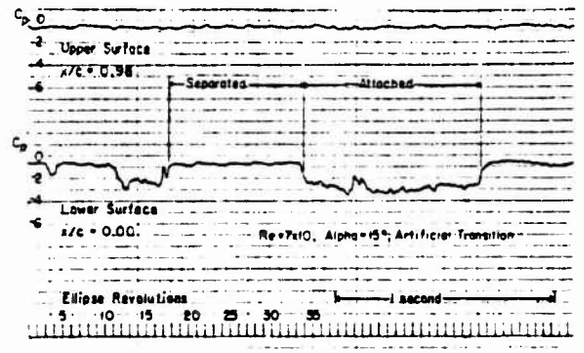

Fig.13 Typical pressure variation with time for the dynamically separated state with artificial transition.

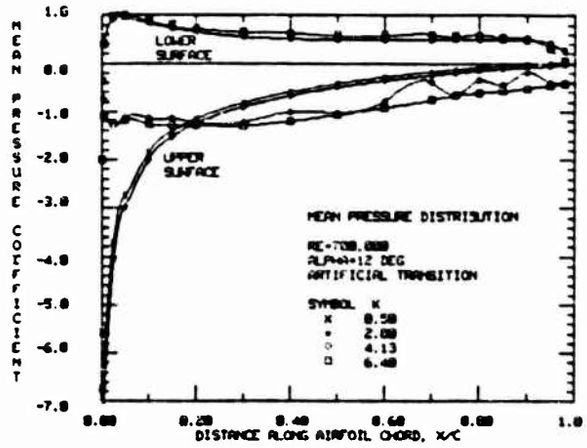

Fig.11 Reduced frequency dependence of the mean pressures at alpha=12 degrees.

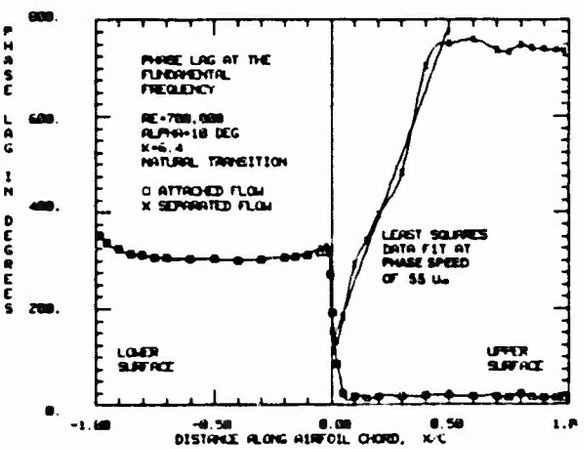

Fig.14 Comparison of phase lag distributions for the attached and separated states.

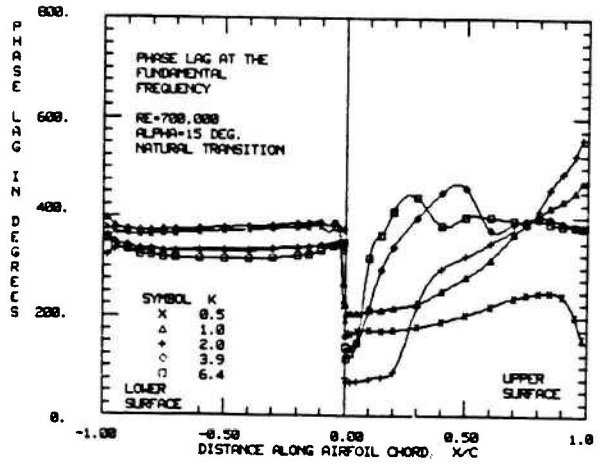

Fig.15 Reduced frequency dependence of the phase lag at alpha=15 degrees.

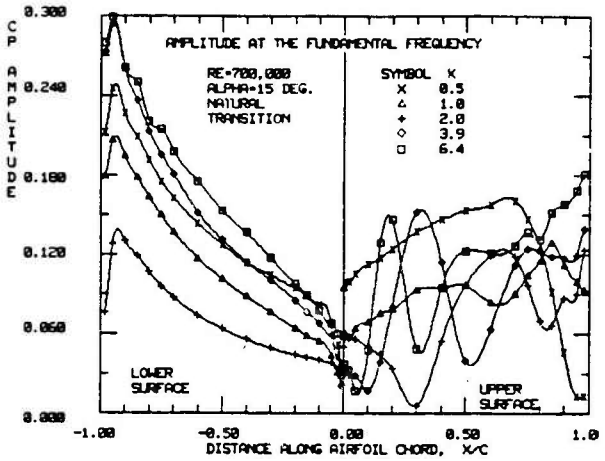

Fig.18 Reduced frequency dependence of the amplitude at alpha=15 degrees.

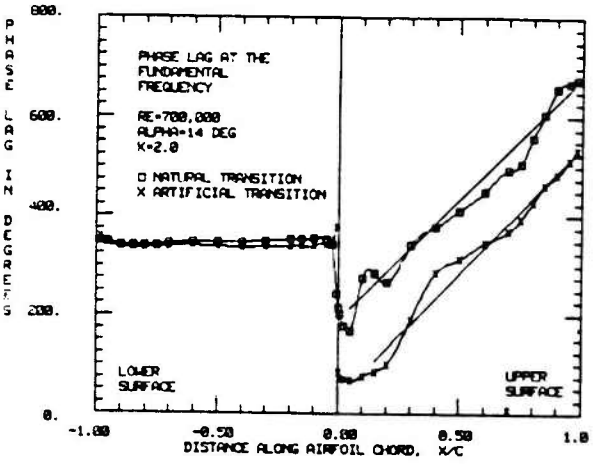

Fig.16 Comparison of the phase lags for natural and artificial transition.

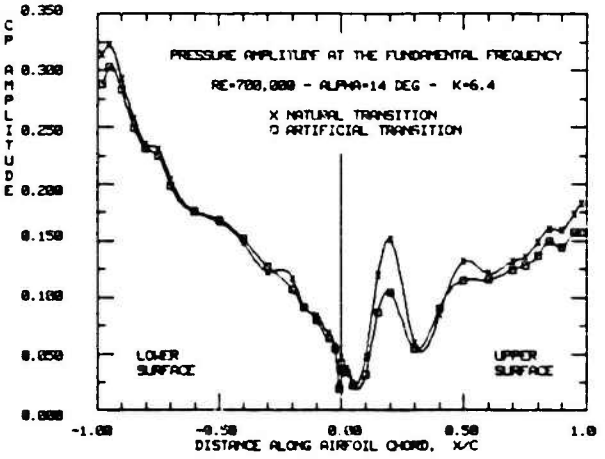

Fig.19 Comparison of the amplitudes for natural and artificial transition.

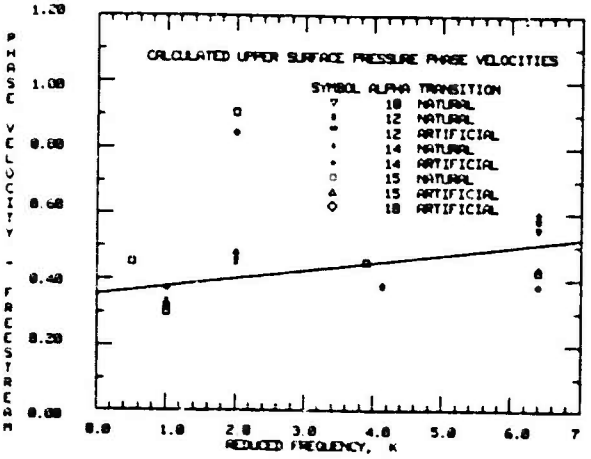

Fig.17 Reduced frequency dependence of the average phase velocity.